

# The Role of Molecular Clusters in the Filling of Carbon Nanotubes

Thomas W. Chamberlain,<sup>†</sup> Andrei M. Popov,<sup>\*</sup> Andrei A. Knizhnik,<sup>§,⊥</sup> Georgii E. Samoilov,<sup>¶</sup> and Andrei N. Khlobystov<sup>†,\*</sup>

<sup>†</sup>School of Chemistry, University of Nottingham, Nottingham, U.K., <sup>‡</sup>Institute of Spectroscopy, 142190, Troitsk, Moscow Region, Russia, <sup>§</sup>Kintech Lab Ltd, 123182, Kurchatov Square, 1, Moscow, Russia, <sup>⊥</sup>RRC "Kurchatov Institute", 123182, Kurchatov Square, 1, Moscow, Russia, and <sup>¶</sup>Moscow Institute of Physics and Technology, 141701, Institutskii per., 9, Dolgoprudny, Moscow Region, Russia

It is well-known that carbon nanotubes can readily absorb different molecules and ions,<sup>1</sup> but the exact mechanism of how the guest-species enter the nanotube host is still debated. Experiments show that molecules can enter nanotubes either from the vapor phase,<sup>2,3</sup> the molten phase (neat compound),<sup>4</sup> or from solution (dissolved compound).<sup>5,6</sup> Although the mechanism of the latter method is least understood, absorption of molecules from solution is becoming increasingly important as it offers a route for insertion of chemically and biologically active molecules into nanotubes.

By contrast, insertion of guest-molecules from the gas phase has been explored in detail for fullerene C<sub>60</sub>.<sup>2,3</sup> It is generally accepted that prior to insertion into the nanotubes, the fullerene guest-molecules become adsorbed on the nanotube surface (Figure 1b) but remain mobile and migrate freely along the nanotube eventually reaching the nanotube terminus (Figure 1c). A moderate activation barrier (~0.3 eV per C<sub>60</sub>) may need to be overcome for the molecule to enter the nanotube, but this energetic penalty is richly compensated upon encapsulation of the molecule (Figure 1d) due to the significantly enhanced van der Waals interactions between the nanotube and the encapsulated molecule (*i.e.*, the nanotube surface wraps around the molecule maximizing the contact area). Clearly, the efficiency of the encapsulation in this case depends critically on the ratio of the nanotube diameter and the diameter of the guest-molecule.<sup>3</sup> Having a perfect geometrical match for the nanotube interior, C<sub>60</sub> interacts strongly with the inside of single-walled carbon nanotubes (SWNT) with a typical diameter of 1.3–1.5 nm.

**ABSTRACT** We have demonstrated that the ability of fullerenes to form clusters is essential for the filling of single-walled carbon nanotubes in solution. In solutions where C<sub>60</sub> exists in the form of discrete solvated molecules (*e.g.*, in CS<sub>2</sub>) no fullerene encapsulation in nanotubes takes place, as the large molar excess of solvent compared to solute prohibits C<sub>60</sub> from entering the nanotubes. However, in solutions containing large clusters of C<sub>60</sub> (*e.g.*, in *n*-hexane) nanotubes become densely filled with fullerene molecules despite the large excess of solvent. The interactions between carbon nanotubes and fullerene clusters provide an efficient transport of C<sub>60</sub> into nanotubes that avoids the detrimental effects of the solvent molecules. This new mechanism provides the first rational explanation of experiments involving nanotube filling with guest-molecules in solution.

**KEYWORDS:** carbon nanotubes · fullerenes · peapod structures · molecular confinement · clusters

Typically vapor phase filling with C<sub>60</sub> leads to high filling rates of up to 100% (*i.e.*, nearly all nanotubes are filled with guest-molecules) as the potential guest-molecules are able to migrate freely, unhindered by other molecules (such as solvent), on the outside and inside of the nanotube. Since fullerene molecules are vaporized in vacuum, the absence of solvent or any other molecules means that the fullerenes can pack closely in the nanotube giving highly ordered arrays of many hundreds of molecules in a row. Unfortunately, the high temperatures required for vaporization (400–600 °C) mean that this method is limited to molecules which are stable to such elevated temperatures and able to sublime readily.

Encapsulation of guest species that neither melt nor sublime has been shown to be possible by immersion of nanotubes with open termini in solutions of these compounds. This provides a way of encapsulating molecules, such as fullerenes functionalized with organic groups<sup>6</sup> or endohedral fullerenes,<sup>7,8</sup> which are unstable to the harsh conditions required for sublimation. The key role of the solvent in this

\*Address correspondence to andrei.khlobystov@nottingham.ac.uk.

Received for review June 8, 2010 and accepted August 26, 2010.

Published online September 10, 2010.  
10.1021/nn101292u

© 2010 American Chemical Society

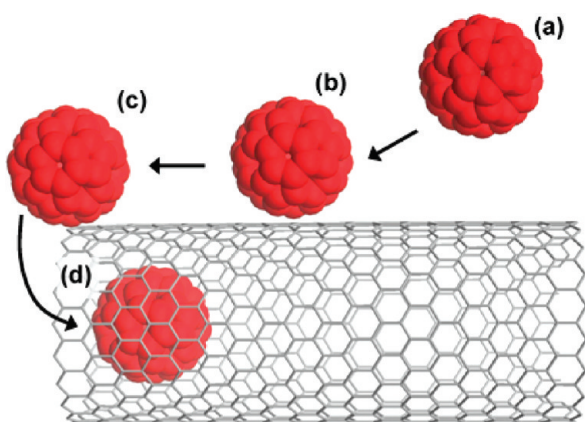


**Figure 1.** Stages of carbon nanotube filling with fullerene  $C_{60}$  via the vapor phase mechanism: (a) fullerene in the gas phase, (b,c) fullerene adsorbed on the nanotube surface diffusing toward the open terminus, (d) fullerene encapsulated inside the nanotube.

mechanism is to enable the transport of guest-molecules from the bulk solution phase into the carbon nanotubes. However, the fate of the thousands of solvent molecules which enter the nanotubes with each guest-molecule remains largely unclear. No viable mechanism of filling carbon nanotubes from the solution phase has been formulated thus far.

Currently, only tentative attempts to provide a model for the transport of fullerenes from conventional and supercritical fluid solutions into carbon nanotubes have been made,<sup>6,7,9</sup> which do not explain the experimental observations entirely. For example,

Simon *et al.* simply compare the state of  $C_{60}$  dissolved in *n*-hexane to that in the gas phase, thus completely disregarding the solvent.<sup>7</sup> Khlobystov *et al.* consider the role of the solvent explicitly and conclude that the physical size of solvent molecules is important for transport of guest-molecules into nanotubes,<sup>6</sup> while Yudasaka *et al.* progress further by emphasizing the importance of the relative strength of the nanotube–fullerene and fullerene–solvent interactions,<sup>9</sup> which gives guidance for choosing the appropriate solvent for solution filling. Despite this progress, none of the previous studies offer any mechanism that provides a satisfactory rationale for the experimental observations. In this study, we report the first full explanation of experiments involving nanotube filling with guest-molecules in solution.

## RESULTS AND DISCUSSION

We have studied the encapsulation of  $C_{60}$  in nanotubes from both carbon disulfide ( $CS_2$ ), a traditionally good fullerene solvent, and *n*-hexane, a poor fullerene solvent. Freshly annealed nanotubes were immersed in the two fullerene solutions and the resultant suspensions were treated with ultrasonic waves to allow the two components to mix thoroughly.<sup>10</sup> The SWNTs were then filtered and washed extensively with  $CS_2$  to remove any unencapsulated fullerene molecules from the outside of the nanotubes. The samples were then analyzed by high resolution transmission electron microscopy (HRTEM), Figure 2.

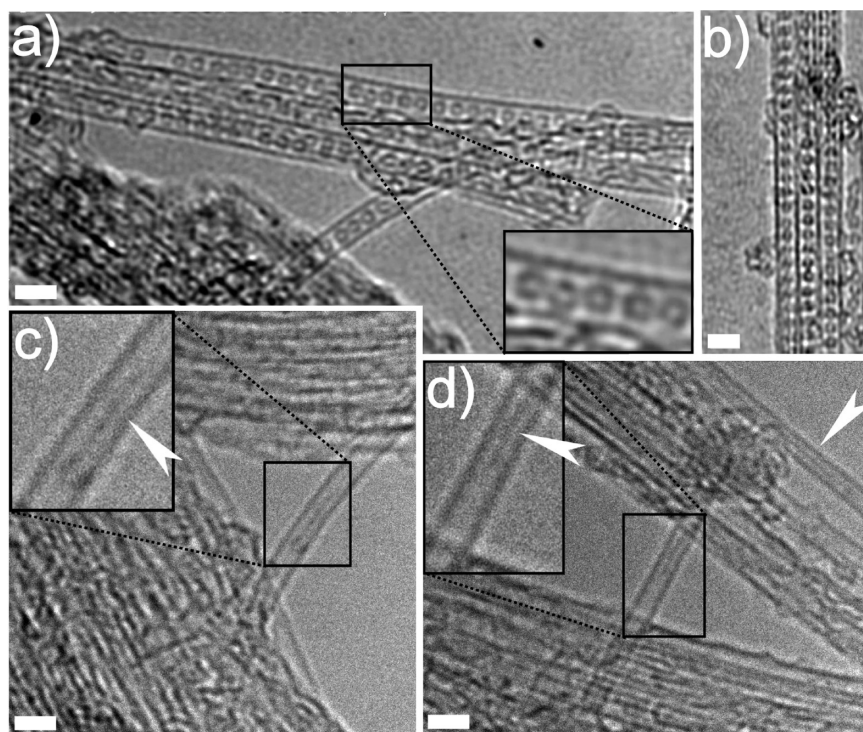


**Figure 2.** HRTEM images of SWNT treated with (a,b) an *n*-hexane solution of  $C_{60}$  and (c,d) a  $CS_2$  solution of  $C_{60}$ . Enlarged regions show (a) fullerene molecules as circles closely packed inside a nanotube, and (c–d) solvent molecules ( $CS_2$ ) inside the nanotube that appear as faint contrast between the nanotube sidewalls (areas highlighted with white arrows). Scale bars = 2 nm.

Extensive HRTEM inspection allows filling rates to be approximated as 60–65% for *n*-hexane solution and <1% for the CS<sub>2</sub> solution. Large numbers of close-packed fullerenes were observed inside nanotubes with no physical gaps between the molecules for SWNT samples immersed in the *n*-hexane solution of C<sub>60</sub>. In comparison, very few fullerenes were found in SWNT immersed in the CS<sub>2</sub> solution of C<sub>60</sub> with no ordered arrays of more than 2 or 3 guest-molecules observed inside the nanotubes. However, the nanotubes are occasionally seen to contain faint contrast features which can be attributed to solvent molecules trapped within the confines of the nanotube (Figure 2c,d). These observations are consistent with previous reports<sup>6,7,9</sup> claiming that insertion of fullerene is only possible from poorly solvating solvents or from supersaturated solutions. It has been suggested that the solvent molecules transport the fullerene molecule to the desired location inside the nanotube then are simply removed when the nanotubes are filtered or dried.<sup>5</sup> However, confinement in the quasi-1D nanotube interior means that it becomes very important to consider the size and shape of solvent molecules used for solution based filling, Figure 3, and the number of solvent molecules per molecule of C<sub>60</sub>, Table 1.

When considering a classical solution of a fullerene species, it is assumed that each fullerene molecule is fully surrounded with a large number of solvent molecules (Figure 4a). According to the Young–Laplace equations, carbon nanotubes immersed in a liquid with a surface tension of below 200 mN/m should be spontaneously filled with this liquid at atmospheric pressure.<sup>11,12</sup> Typically, solvents used for dissolving fullerene have a surface tension that is far below 200 mN/m and can therefore enter into carbon nanotubes together with the guest-molecules of the compound intended to be encapsulated.

In fullerene solutions (Table 1) the molar ratio of solvent to solute is very high, which means that even in very concentrated solutions there will be tens of thousands of solvent molecules per molecule of C<sub>60</sub>. Statistically, it is more likely for solvent molecules to enter the nanotube first (Figure 4b). The interaction between the solvent molecule and the inner wall of the nanotube is significantly lower than that for C<sub>60</sub> so solvent molecules are able to move freely in and out of the nanotube at room temperature (Figure 4b). However, when an individual fullerene molecule enters a nanotube (Figure 4c,d) it forms strong van der Waals interactions with the nanotube interior (3 eV)<sup>2,3</sup> meaning that the encapsulation process of a fullerene molecule is irreversible. In the case of the CS<sub>2</sub> solution, there will be thousands of molecules of solvent for every C<sub>60</sub> present in the system. Therefore, each SWNT, which have a typical length of 2–5 μm in our experiments, will absorb on average only a small number (<10) of molecules of C<sub>60</sub> from the CS<sub>2</sub> solution. This explains the extremely

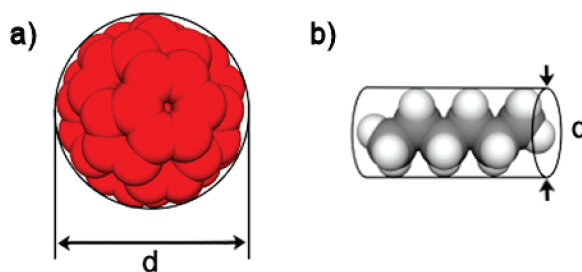


Figure 3. (a) Fullerene molecule and (b) *n*-hexane molecule both with a black circle illustrating their critical dimension, *d*.

poor filling rate of SWNT which were immersed in CS<sub>2</sub> solutions of fullerene and the presence of faint, diffuse features within the nanotubes observed by HRTEM which can be attributed to numerous CS<sub>2</sub> molecules tumbling inside the SWNT.

The fact that nanotubes immersed in *n*-hexane solutions of C<sub>60</sub> become densely filled with fullerenes appears to contradict the nanotube filling mechanism described above. Since there are nearly twice as many solvent molecules per C<sub>60</sub> in the *n*-hexane solution as compared to CS<sub>2</sub>, the filling rate of the SWNT with fullerenes is expected to be significantly lower for *n*-hexane. Indeed, the internal channels of the nanotubes are expected to be filled predominantly with *n*-hexane with almost no C<sub>60</sub> present. This is in a stark contrast to our experimental observations (Figure 2a,b). The only possible explanation for the presence of large numbers of C<sub>60</sub> in the nanotubes is that in solution *fullerenes interact with SWNT not as discrete molecules but as large clusters of molecules*. Fullerenes have a very limited solubility in *n*-hexane (Table 1) as a result of their low affinity for alkane molecules, and hence it is energetically more favorable for C<sub>60</sub> molecules to form clusters in the *n*-hexane solution due to attractive inter-fullerene van der Waals interactions (Figure 6a). The high cohesive energy of fullerene clusters (~2 eV)<sup>13</sup> outweighs the weak solvation energy of the poor solvent (*n*-hexane) leading to the formation of fullerene clusters in the liquid phase. Dynamic light scattering (DLS) measurements of a solution of C<sub>60</sub> in *n*-hexane clearly demonstrate the presence of fullerene clusters (Figure 5).

TABLE 1. Solubility of C<sub>60</sub>,<sup>14</sup> the Mole Fraction of C<sub>60</sub> in a Variety of Saturated Solutions and the Critical Dimension of the Individual Solvent Molecules (Critical Dimension of C<sub>60</sub> Is 1 nm)

solvent	solubility of C <sub>60</sub> /g L <sup>-1</sup>	molar ratio of C <sub>60</sub>	critical dimension of solvent/nm
carbon disulfide	7.9	$6.6 \times 10^{-4}$	0.36
toluene	2.8	$4 \times 10^{-4}$	0.67
<i>o</i> -dichlorobenzene	27	$5.3 \times 10^{-4}$	0.78
ethanol	0.001	$1 \times 10^{-7}$	0.44
carbon dioxide	unknown	unknown	0.28
chloroform	1.5	$3.6 \times 10^{-4}$	0.51
<i>n</i> -hexane	0.043	$1.2 \times 10^{-4}$	0.44



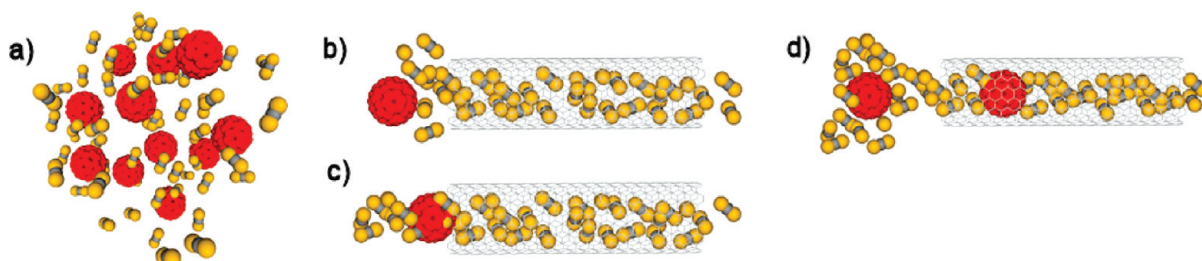


**Figure 4.** (a) Individual  $C_{60}$  molecules dissolved in  $CS_2$ , (b–d) the sequential steps of the encapsulation process of  $C_{60}$  molecules from  $CS_2$  solution into a SWNT. Solvent molecules are present in a large excess as compared to  $C_{60}$ , and therefore, are more likely to enter the nanotube first (b), followed by a single fullerene molecule (c). Thousands of solvent molecules are then expected to enter the SWNT after the initial fullerene (d), which will become trapped by a second fullerene, creating large gaps between individual fullerenes inside the nanotube. (Note, in reality up to 66 000  $CS_2$  molecules will be separating the two closest fullerenes in the nanotube and therefore, on average, each nanotube in our experiment is expected to encapsulate only one  $C_{60}$ ).

The *n*-hexane solution is shown to contain fullerene aggregates of around 255 nm in diameter; this corresponds to clusters containing approximately 8.5 million  $C_{60}$  molecules. When the molecular clusters are removed from the solution by filtration (membrane filter, pore size 200 nm), UV–vis spectroscopy shows a 1000-fold decrease in the concentration of fullerene remaining in the filtrate. This confirms that in the *n*-hexane solution used for filling nanotubes 99.9% of  $C_{60}$  molecules exist in the form of clusters. The existence of metastable fullerene clusters in supersaturated solutions is also well documented;<sup>15–20</sup> however, the connection between this phenomenon and nanotube filling mechanisms has never been made.

In contrast, the solution of  $C_{60}$  in  $CS_2$  does not contain any fullerene clusters (*i.e.*, only fully solvated  $C_{60}$  molecules are present) with no species of greater than 1 nm detected (additional DLS and UV–vis data is included in S5, Supporting Information file).

When nanotubes are immersed in a solution containing  $C_{60}$  clusters, the solvent is free to enter and leave the nanotube as before (Figure 6b). However, eventually a fullerene cluster will come into contact with the end of a nanotube (Figure 6c) and one of the fullerene molecules will enter the nanotube becoming irreversibly encapsulated.

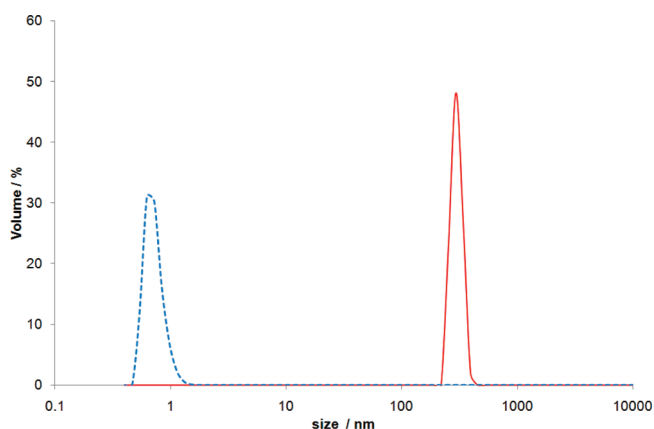


**Figure 5.** DLS measurements for solution of  $C_{60}$  in *n*-hexane (solid line) and  $CS_2$  (dotted line), showing the presence of fullerene clusters in the *n*-hexane solution.

Solvent molecules within the nanotube are now prevented from leaving the nanotube from that end by the fullerene cluster but are free to leave from the other end of the nanotube. The fullerene cluster is expected to be attached firmly to the nanotube, as fullerenes are attracted strongly to the nanotube surface and to each other by van der Waals forces which are particularly significant in a weakly solvating solvent.<sup>21</sup> As long as the fullerene cluster remains in this “docking” position (Figure 6d,e) no surrounding solvent molecules can enter the nanotube. The fullerenes within the cluster will proceed one by one into the nanotube driven by the large energy gained upon encapsulation (Figure 6d), while the solvent molecules, interacting with the nanotube only weakly, will be driven out through the other end of the nanotube. This will result in a continuous array of fullerenes with no solvent molecules between the individual fullerene cages (Figure 6e) as observed by HR-TEM. Clearly, the successful encapsulation of fullerenes is only possible if the nanotube is open at both ends and has no internal obstructions to the solvent/fullerene moving inside. Therefore, only relatively short and structurally perfect nanotubes can be filled in solution which significantly lowers the filling rate of solution methods (typically 30–70%) as compared with the gas phase methods (80–100%).

If the proposed mechanism is considered a diffusion-limited process<sup>22</sup> the average time needed for a cluster of fullerenes to collide with the entrance of a stationary SWNT in solution can be expressed as:

$$t = (4\pi\gamma DRn)^{-1}$$

where  $n$  is the concentration of clusters in solution,  $D$  is the diffusion coefficient of the cluster,  $R$  is the cluster radius, and  $\gamma$  is a factor taking into account that collisions can occur at the two ends of the nanotube. This estimation shows that the time required for collision between the fullerene clusters observed in our experiments and the nanotube entrance is significantly shorter (5 min) than the duration of the experiment (3 h). Consideration of the mobility of the nanotubes would further decrease the estimated time of collision (S2, Supporting Information).

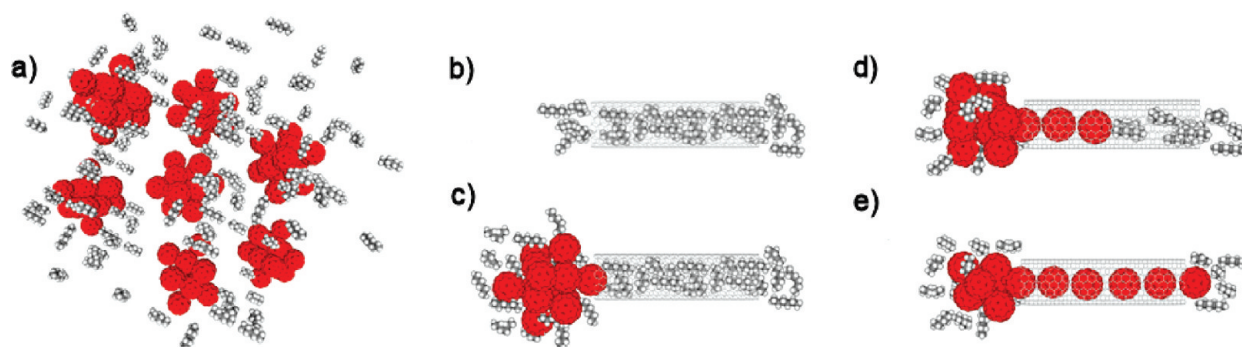


Figure 6. (a) Clusters of  $C_{60}$  in *n*-hexane, (b–e) the sequential steps of the encapsulation process of  $C_{60}$  molecules from *n*-hexane. Solvent molecules enter the nanotube first (b), followed by a cluster of fullerenes making contact with the open end of a SWNT (c). Fullerenes from the cluster enter the nanotube one-by-one (d,e), while the solvent molecules are expelled from the opposite end of the nanotube.

To investigate the energy pathway by which individual fullerene  $C_{60}$  molecules transfer from a fullerene cluster directly into the interior of a nanotube, interactions of a (10,10) nanotube with fullerene clusters of different sizes corresponding to the range  $N_m = 13–1282$  molecules have been studied. Our theoretical modeling showed that the surface of fullerene clusters is highly heterogeneous, containing surface molecules with coordination numbers ranging from four to nine which is in agreement with previous investigations of the structure of small fullerene clusters.<sup>23</sup> The mean coordination number of surface molecules  $\langle N_c \rangle$  in clusters of medium size  $N_m \approx 100–200$  is practically the same as that in large fullerene clusters  $N_m \approx 1000$  (S1, Supporting Information), thus indicating that in these models  $\langle N_c \rangle$  approaches a value for macroscopically large clusters. Also, it should be noted that the radius of a cluster of  $N_m \approx 1000$  fullerenes is already significantly greater than the

distance between neighboring molecules within the cluster interacting with each other *via* short-range attractive forces. Therefore, the interactions of a nanotube with an  $N_m \approx 1000$  cluster of fullerenes should be very close to those for the much larger  $N_m \approx 10^7$  clusters observed experimentally.

To account for the inhomogeneity of the cluster surface we explored encapsulation pathways for fullerenes with different coordination numbers from clusters of different sizes. The energy of the encapsulation pathway was scanned with a constrained optimization, in which a single fullerene was shifted in steps of 0.02 nm from the fullerene cluster toward the interior of the nanotube and the positions of all of the remaining molecules in the cluster were optimized at each step. The key parameters of the pathway (Figure 7) are the barrier for the transfer of a fullerene from a cluster to a nanotube ( $E_a$ ) and the total energy gain upon encapsulation of the molecule ( $E_t$ ). These parameters were ob-

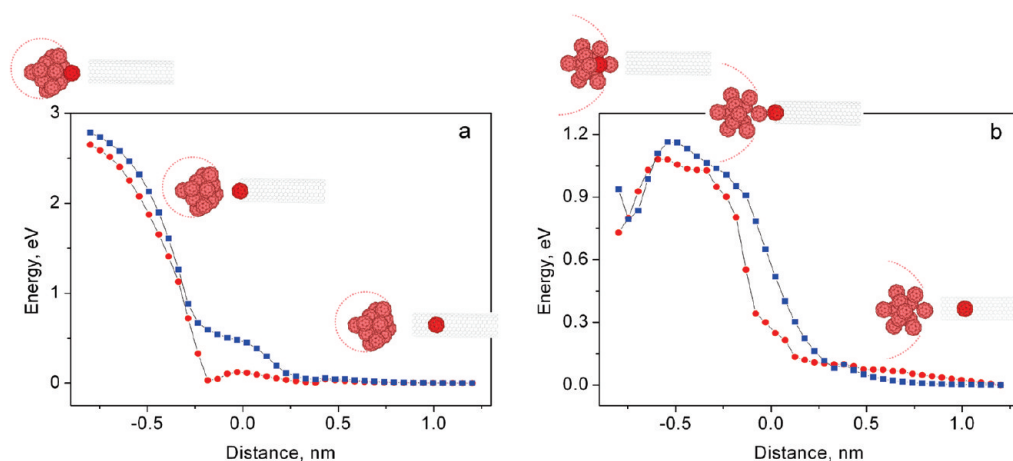


Figure 7. Calculated energy profiles for the transfer process of a fullerene molecule from fullerene clusters into a (10,10) nanotube. (a) For “smaller” clusters the transfer proceeds without an activation barrier, illustrated for a fullerene with a coordination number of 6 from a  $(C_{60})_{13}$  cluster (squares) and for a fullerene with a coordination number of 4 from a  $(C_{60})_{144}$  cluster (circles). (b) In “larger” clusters the transfer proceeds with an activation barrier, illustrated for a fullerene with a coordination number of 8 from a  $(C_{60})_{171}$  cluster (squares) and from a  $(C_{60})_{1282}$  cluster (circles). The potential energy of the  $C_{60}$  molecule is plotted as a function of distance between the center of the fullerene (red) and the edge of the nanotube. The zero potential energy in each system corresponds to the case where one fullerene is fully encapsulated inside the nanotube. Diagrammatic representations refer to the position of the fullerene in relation to the nanotube along the encapsulation pathway having left the fullerene cluster (as only a portion of the fullerene cluster is shown, a pink dashed line schematically outlines the boundary of the cluster).

tained for all calculated energies of the encapsulation pathway (S1, Supporting Information).

The transfer of fullerenes into a nanotube without any barrier appears to be possible only for small molecular clusters,  $N_m \approx 10-50$ , or for fullerenes with a coordination number  $N_c = 4$  from the surface of a larger cluster ( $C_{60}$ )<sub>144</sub> (Figure 7a). For very large clusters, such as ( $C_{60}$ )<sub>1282</sub>, the transfer of any surface fullerene into a nanotube takes place with a barrier  $E_a$  of about 0.35 eV, which is virtually independent of the coordination number (S1, Supporting Information).

Although DLS measurements show that a distribution of different fullerene clusters exists in *n*-hexane with an average cluster size of 8.5 million molecules, the activation energy for a fullerene molecule to escape from a cluster does not depend on cluster size (S1, Supporting Information). Figure 7b shows that for larger clusters the key energetic parameters,  $E_a$  and  $E_v$ , vary only slightly. Therefore, even though the experimentally observed clusters are significantly larger than those considered in the calculation, the results of the theoretical calculations are directly applicable to our experimental observations. In contrast to the energetic barrier depending only weakly on the coordination number of the surface molecule, the energy gain,  $E_v$ , appears to decrease with the coordination number, asymptotically approaching 0.7 eV for  $C_{60}$  in very large clusters.

Using the above energetic parameters it is also possible to estimate the average time for the transfer of one fullerene molecule from a fullerene cluster into a nanotube using the Arrhenius formula:

$$t^{-1} = \nu_0 \exp\left(-\frac{E_a}{kT}\right)$$

where  $E_a$  is the activation barrier and  $\nu_0$  is the pre-exponential multiplier which has the same order of magnitude as the frequency of oscillation of the fullerene in the cluster that is closest to the open end of the nanotube. According to the MD simulation this frequency ( $\nu_0$ ), is approximately  $6 \times 10^{11} \text{ s}^{-1}$  for the largest cluster ( $C_{60}$ )<sub>1282</sub>. For  $\nu_0 \approx 10^{12} \text{ s}^{-1}$  and  $E_a = 0.35 \text{ eV}$  at  $T = 300 \text{ K}$ , it is estimated that the average time for the transfer of one fullerene molecule into a nanotube is  $\sim 10^{-6} \text{ s}$ . This time is much shorter than the time required for the collision between the fullerene clusters and nanotubes to occur (300 s), and is substantially shorter than the duration of the nanotube filling experiment (3 h).

The calculations show that regardless of the size of the large clusters, the activation barrier for the transfer of a fullerene into the nanotube reaches a plateau in the

region of 0.35 eV (Figure 7). This barrier is very close to the barrier of 0.37 eV reported for insertion of  $C_{60}$  molecules preadsorbed on the SWNT surface (Figure 1b), which is known to lead to a spontaneous and irreversible encapsulation of fullerenes.<sup>2</sup> The energy of 0.7 eV gained upon transfer and encapsulation of each  $C_{60}$  is sufficiently high and the transfer time of  $10^{-6} \text{ s}$  per  $C_{60}$  is sufficiently short to enable efficient filling of carbon nanotubes directly from fullerene clusters docked at the nanotube termini. Mechanical mixing of macroscopic crystals of fullerene and nanotubes without solvent in principle also allows transport and encapsulation of the guest-molecules directly from the crystals into the nanotube (S4, Supporting Information), but the yield of this process is very low due to polymerization of fullerenes caused by the mechanical activation. An alternative route for the cluster-to-nanotube transfer process to occur would involve the adsorption of fullerene clusters on the SWNT sidewalls followed by a surface diffusion of individual fullerene molecules into the nanotubes. However, this pathway appears to be energetically significantly less favorable than the direct docking mechanism (S3, Supporting Information file).

## CONCLUSIONS

Methods for the insertion of molecules into carbon nanotubes from the solution phase have become increasingly more important as the demand for novel optically, magnetically, and biologically active molecules confined within SWNT is rapidly increasing.<sup>24</sup> Previously, we and others have demonstrated that the nature of the solvent is crucial for the molecular encapsulation process.<sup>5-7,9</sup> The filling of nanotubes with fullerenes was significantly more efficient for weakly solvating solvents, such as *n*-hexane, ethanol, or supercritical  $\text{CO}_2$ , than for good fullerene solvents, such as toluene, *o*-dichlorobenzene or  $\text{CS}_2$ . Up until now, these experimental facts have been in contradiction with the current understanding of fullerene–nanotube interactions. We have demonstrated experimentally that in solution fullerenes interact with nanotubes not as individual discrete molecules, but as large clusters of molecules. Theoretical modeling indicates that the rate of nanotube filling in solution is limited by the diffusion of fullerene clusters toward the nanotube termini. Consideration of fullerene clusters in the nanotube filling mechanisms for the first time provides a satisfactory explanation for experimental observations and opens new avenues for the assembly of molecular architectures in carbon nanotubes.

## EXPERIMENTAL METHODS

Encapsulation experiments were carried out using arc-discharge produced SWNT (NanoCarbLab) and  $C_{60}$  (SES Research). All other reagents and solvents were purchased from Sigma-Aldrich Chemicals and were used without further purification.

The following procedure was used for each filling experiment:

Purified SWNT (3 mg) were annealed in air at 520 °C for 15 min and then kept at 400 °C to avoid the presence of water in the sample. A 3-fold excess of fullerene (4 mg) was dispersed/

dissolved in the chosen solvent (4 mL of *n*-hexane or CS<sub>2</sub>; a stable supersaturated solution is formed in *n*-hexane) using ultrasonic waves, the freshly annealed SWNTs were added, and the resultant suspensions were treated with ultrasonic waves for 3 h. The suspension was then filtered and washed with CS<sub>2</sub> (20 mL) to remove any fullerenes adsorbed on the surface of the nanotubes and then with methanol (20 mL).

Transmission electron microscopy analysis was performed using JEOL-2100F field-emission gun and JEOL-4000EX LaB<sub>6</sub> microscopes. The imaging conditions were carefully tuned by lowering the accelerating voltage of the microscope to 100 kV and reducing the beam current density to a minimum. Nanotube samples (2–3 mg) were dispersed in 2 mL of methanol using an ultrasonic bath and deposited onto lacy carbon-film-coated TEM copper grids. The filling rates were determined by taking micrographs of 100 × 100 nm<sup>2</sup> areas from different regions of the specimen and estimating the proportion of filled nanotubes for each area. By averaging the filling factors over 50–70 areas it is possible to obtain a good representation of the composition of each sample.<sup>6</sup>

DLS measurements were performed using a Malvern Instruments Nano-ZS Zetasizer at room temperature. C<sub>60</sub> (5 mg) was dispersed in CS<sub>2</sub> or *n*-hexane (5 mL) using sonication, and the resultant solution/suspension was allowed to equilibrate for 10 min. Average particle diameters (APD) are quoted in units of nm. Quoted values are the average of 3 measurements. C<sub>60</sub> (CS<sub>2</sub> solution): APD = 0.66 ± 0.19 nm, C<sub>60</sub> (*n*-hexane solution): APD = 255 ± 18.62 nm. Filtration of the *n*-hexane solution through a PTFE membrane filter (pore size 200 nm) removes all the clusters observed in DLS, which correspond to 99.9% of fullerene in the original solution.

**Theoretical Methods.** To investigate the interaction of fullerene clusters with empty carbon nanotubes a coarse grained model was developed in which each fullerene is represented as a single point with effective potential. For fullerene–fullerene interactions we used a pair potential introduced by Girifalco:<sup>25</sup>

$$V(r_{ij}) = -\alpha \left[ \frac{1}{s(s-1)^3} + \frac{1}{s(s+1)^3} - \frac{2}{s^4} \right] + \beta \left[ \frac{1}{s(s-1)^9} + \frac{1}{s(s+1)^9} - \frac{2}{s^{10}} \right]$$

where  $r_{ij}$  is the distance between the centers of two fullerenes,  $s = r_{ij}/(2a)$  and  $a$  is the C<sub>60</sub> fullerene radius (0.355 nm). This potential was obtained by integrating the Lennard-Jones 12-6 potential ( $U = 4\epsilon((\sigma/r)^{12} - (\sigma/r)^6)$ ) interaction for two perfect spheres whose surfaces consist of a uniform density of carbon atoms. For a fullerene–fullerene interaction the potential has the following parameters;  $\alpha = N^2\epsilon/3(\sigma/2a)^6$  and  $\beta = N^2\epsilon/18(\sigma/2a)^{12}$ , where  $N$  is the number of carbon atoms in the fullerene. A bicubic spline interpolation was used to approximate the fullerene–nanotube interaction using the potential energy obtained by numerical summation of a pair of interatomic interaction energies described by the Lennard-Jones 12-6 potential. The parameters  $\epsilon = 2.86$  meV and  $\sigma = 0.3466$  nm of the Lennard-Jones potential were used for the fullerene–fullerene interaction.<sup>25</sup> The parameters  $\epsilon = 2.62$  meV and  $\sigma = 0.344$  nm were used for the fullerene–nanotube interaction.<sup>26</sup> The cutoff distance of the Lennard-Jones potential was chosen to be 0.12 nm.

In the MD simulations the time step was 6 fs, which is about 100 times smaller than the period of thermal vibrations of fullerenes inside the cluster. The temperature of the coarse-grained system was controlled using a velocity rescaling algorithm.

**Acknowledgment.** This work was supported by the University of Nottingham, the Engineering and Physical Sciences Research Council (EPSRC), the European Science Foundation, and the Royal Society. We are grateful to G. Rance for his assistance with DLS measurements and to the Nottingham Nanoscience and Nanotechnology Centre for access to TEM facilities. This work was in part supported by the Russian Foundation for Basic Research, Grants 08-02-00685.

**Supporting Information Available:** Full details of all theoretical calculations performed, a complete set of DLS data, and experimental detail for nanotube filling experiments in the solid state. This material is available free of charge via the Internet at <http://pubs.acs.org>.

## REFERENCES AND NOTES

1. Khlobystov, A. N. Endohedral Modification of Carbon Nanotubes. In *Chemistry of Carbon Nanotubes*; Basiuk, V. A., Basiuk, E. V., Eds.; American Scientific: Stevenson Ranch, CA, 2008; Vol. 3, pp 87–111.
2. Ulbricht, H.; Moos, G.; Hertel, T. Interaction of C<sub>60</sub> with Carbon Nanotubes and Graphite. *Phys. Rev. Lett.* **2003**, *90*, 095501.
3. Girifalco, L. A.; Hodak, M. Van der Waals Binding Energies in Graphitic Structures. *Phys. Rev. B* **2002**, *65*, 125404.
4. Costa, P. M. F. J.; Friedrichs, S.; Sloan, J.; Green, M. L. H. Imaging Lattice Defects in Alkali-Metal Halides Encapsulated within Double Walled Carbon Nanotubes (DWNTs). *Chem. Mater.* **2005**, *17*, 3122–3129.
5. Liu, Z.; Yanagi, K.; Suenaga, K.; Kataura, H.; Iijima, S. Imaging the Dynamic Behaviour of Individual Retinal Chromophores Confined inside Carbon Nanotubes. *Nat. Nanotechnol.* **2007**, *2*, 422–425.
6. Khlobystov, A. N.; Britz, D. A.; O'Neil, A. S.; Wang, J.; Poliakov, M.; Briggs, G. A. D. Low Temperature Assembly of Fullerene Arrays in Single-Walled Carbon Nanotubes Using Supercritical Fluids. *J. Mater. Chem.* **2004**, *14*, 2852–2857.
7. Simon, F.; Kuzmany, H.; Rauf, H.; Pichler, T.; Bernardi, J.; Peterlik, H.; Korecz, L.; Fulop, F.; Janossy, A. Low Temperature Fullerene Encapsulation in Single Wall Carbon Nanotubes: Synthesis of NC<sub>60</sub>SWCNT. *Chem. Phys. Lett.* **2004**, *383*, 362–367.
8. Corzilius, B.; Gembus, A.; Weiden, N.; Dinse, K. -P.; Hata, K. EPR Characterization of Catalyst-Free SWNT and N@C<sub>60</sub>-Based Peapods. *Phys. Stat. Sol. (b)* **2006**, *243* (13), 3273–3276.
9. Yudasaka, M.; Ajima, K.; Suenaga, K.; Ichihashi, T.; Hashimoto, A.; Iijima, S. Nano-Extraction and Nano-Condensation for C<sub>60</sub> Incorporation into Single-Wall Carbon Nanotubes in Liquid Phases. *Chem. Phys. Lett.* **2003**, *380*, 42–46.
10. In our experiments, the extent to which the SWNT are bundled together is the same in both solvents. The encapsulation energy for a fullerene molecule entering an individual SWNT is expected to be the same for an isolated SWNT as for a SWNT contained within a bundle.
11. Pederson, M. R.; Broughton, J. Q. Nanocapillarity in Fullerene Tubules. *Phys. Rev. Lett.* **1992**, *69*, 2689–2692.
12. Dujardin, E.; Ebbesen, T. W.; Hiura, H.; Taginaki, K. Capillarity and Wetting of Carbon Nanotubes. *Science* **1994**, *265*, 1850–1852.
13. Lu, J. P.; Li, X. P.; Martin, R. M. Ground State and Phase Transitions in Solid C<sub>60</sub>. *Phys. Rev. Lett.* **1992**, *68*, 1551–1554.
14. Ruoff, R. S.; Tse, D. S.; Malhotra, R.; Lorents, D. S. Solubility of C<sub>60</sub> in a Variety of Solvents. *J. Phys. Chem.* **1993**, *97*, 3379–3383.
15. Tomiyama, T.; Uchiyama, S.; Shinohara, H. Solubility and Partial Specific Volumes of C<sub>60</sub> and C<sub>70</sub>. *Chem. Phys. Lett.* **1997**, *264*, 143–148.
16. Ghosh, H. N.; Sapre, A. V.; Mittal, J. P. Aggregation of C<sub>70</sub> in Solvent Mixtures. *J. Phys. Chem.* **1996**, *100*, 9439–9443.
17. Sun, Y. -P.; Bunker, C. E. C<sub>70</sub> in Solvent Mixtures. *Nature* **1993**, *365*, 398.
18. Sun, Y. -P.; Ma, B.; Bunker, C. E.; Liu, B. All-Carbon Polymers (Polyfullerenes) from Photochemical Reactions of Fullerene Clusters in Room-Temperature Solvent Mixtures. *J. Am. Chem. Soc.* **1995**, *117*, 12705–12711.
19. Bezmelnitsin, V. N.; Eletsii, A. V.; Stepanov, E. V. Cluster Origin of Fullerene Solubility. *J. Phys. Chem.* **1994**, *98*, 6665–6667.

20. Nath, S.; Pal, H.; Sapre, A. V. Effect of Solvent Polarity on the Aggregation of Fullerenes: A Comparison Between  $C_{60}$  and  $C_{70}$ . *Chem. Phys. Lett.* **2002**, *360*, 422–428.
21. Khlobystov, A. N.; Porfyrakis, K.; Britz, D. A.; Kanai, M.; Scipioni, R.; Lyapin, S. G.; Wiltshire, J. G.; Ardavan, A.; Nguyen-Manh, D.; Nicholas, R. J.; *et al.* Ordering and Interaction of Molecules Encapsulated in Carbon Nanotubes. *Mater. Sci. Technol.* **2004**, *20*, 969–974.
22. Smoluchowski, M. V. Drei Vorträge über Diffusion, Brownsche Bewegung und Koagulation von Kolloidteilchen. *Phys. Z.* **1916**, *17*, 557–585.
23. Doye, J. P. K.; Wales, D. J.; Branz, W.; Calvo, F. Modeling the Structure of Clusters of  $C_{60}$  Molecules. *Phys. Rev. B* **2001**, *64*, 235409.
24. Furukawa, K.; Okubo, S.; Kato, H.; Shinohara, H.; Kato, T. High-Field/High-Frequency ESR Study of  $Gd@C_{82}$ -I. *J. Phys. Chem. A* **2003**, *107*, 10933–10937.
25. Girifalco, L. A. Molecular-Properties of  $C_{60}$  in the Gas and Solid-Phases. *J. Phys. Chem.* **1992**, *96*, 858–861.
26. Girifalco, L. A.; Hodak, M.; Lee, R. S. Carbon Nanotubes, Buckyballs, Ropes, and a Universal Graphitic Potential. *Phys. Rev. B* **2000**, *62*, 13104.